Astron. Astrophys. 348, 614–620 (1999)

ASTRONOMY AND ASTROPHYSICS

A heliospheric density model and type III radio bursts

G. Mann[1], **F. Jansen**[1], **R.J. MacDowall**[2], **M.L. Kaiser**[2], **and R.G. Stone**[2]

[1] Astrophysikalisches Institut Potsdam, An der Sternwarte 16, D-14482 Potsdam, Germany
[2] NASA/Goddard Space Flight Center, Code 695, Greenbelt, MD 20771, USA

Received 17 November 1997 / Accepted 8 February 1999

Abstract. A heliospheric density model is derived by evaluating the spherical solutions of magnetohydrostatic equations including the thermal pressure and the gravitational force of the Sun. The model resulting as a special solution of Parker's wind equation covers a range from the low corona up to 5 AU and, surprisingly, agrees very well with observations. Such a model is required for the interpretation of solar and interplanetary radio observations since the emission of the radio radiation is regarded to be generated near the local electron plasma frequency, which depends on the electron number density. Thus, the density model yields the radial distance of the radio source from the Sun and, consequently, the radial source velocity from the drift in dynamic radio spectra. The model is applied for estimating the velocity of electron beams generating solar and interplanetary type III radio bursts.

Key words: Magnetohydrodynamics (MHD) – Sun: corona – Sun: magnetic fields – Sun: radio radiation – inteplanetary medium

1. Introduction

Generally, the solar and interplanetary radio radiation is considered to be generated by plasma emission. In such processes, suprathermal electrons excite high frequency electrostatic waves (e. g. Langmuir waves and upper hybrid waves), which convert into electromagnetic (radio) waves by nonlinear interaction with low frequency plasma waves and/or scattering off ion density fluctuations (Melrose 1985). This mechanism is responsible for the fundamental radiation. Furthermore, the coalescence of two high frequency electrostatic plasma waves leads to the harmonic emission (Melrose 1985). Thus, the radio waves are emitted near the local electron plasma frequency $f_{pe} = (e^2 N/\pi m_e)^{1/2}$ (e, elementary charge; N, electron number density; m_e, electron mass) or its harmonics. Then, high frequency radio waves (e. g. 400 MHz) are generated in the low corona, while the low frequency waves (e. g. 20 kHz) are emitted from sources roughly located at 1 AU (1 AU = $150 \cdot 10^6$ km). A radial motion of a radio source would appear as a drift in the corresponding dynamic radio spectrum. The relationship between the drift rate D_f measured at the frequency f and the radial source velocity V_r is given by

$$D_f = \frac{f}{2} \cdot \frac{1}{N} \cdot \frac{dN}{dr} \cdot V_r \qquad (1)$$

Such radio sources are sub-relativistic electron beams and travelling shock waves, for instance, appearing as type III and II bursts in dynamic radio spectra, respectively (cf. e. g., Suzuki & Dulk (1985) and Gurnett (1995) as reviews). The knowledge of a heliospheric density model would provide the distance of the radio source from the Sun. Consequently, the radial velocity of the radio source can be deduced from the drift rate of the associated radio signature in dynamic radio spectra according to (1). These facts illustrate the importance of the knowledge of a heliospheric density model.

The heliosphere is highly structured, i. e., it is filled by high and low speed solar wind streams, the so-called heliospheric current sheet, corotating interaction regions and travelling disturbances (e. g. coronal mass ejections and interplanetary shocks) (cf. e. g. Schwenn (1990) as a review). Because of these reasons, a global radial density model of the heliosphere is an approximation. Nevertheless, such a global model would be useful for the interpretation of solar and interplanetary radio data as presently received by the instruments URAP (Stone et al. 1992) and WAVES (Bougeret et al. 1995) aboard the spacecrafts ULYSSES and WIND, respectively. Therefore, we derive a heliospheric density model, which is an average but in agreement with observations between the low corona and 5 AU.

In Sect. 2 the heliospheric density model is derived by means of the magnetohydrostatic equations supplemented by an isothermal equation of state and the gravitational force of the Sun. The resulting density model is compared with different measurements of the density in the low corona and the interplanetary space in Sect. 3. Finally, the model is applied for estimating the velocities of energetic electrons associated with the solar and interplanetary type III radio bursts on December 27, 1994.

2. Derivation of the heliospheric density model

In order to derive the required heliospheric density model the magnetohydrodynamic equations

$$0 = \frac{\partial \rho}{\partial t} + div(\rho \boldsymbol{v}) \qquad (2)$$

Send offprint requests to: G. Mann (GMann@aip.de)

$$\rho \cdot \left[\frac{\partial \boldsymbol{v}}{\partial t} + (\boldsymbol{v} \cdot \boldsymbol{\nabla}) \right] = -\boldsymbol{\nabla} p - \frac{1}{4\pi} (\boldsymbol{B} \times rot \boldsymbol{B}) + \boldsymbol{f} \quad (3)$$

$$\frac{\partial \boldsymbol{B}}{\partial t} = rot\,(\boldsymbol{v} \times \boldsymbol{B}) \quad (4)$$

are employed with the velocity $\boldsymbol{v}$ of flow, the mass density ρ, the thermal pressure p, the magnetic field $\boldsymbol{B}$, and the external force $\boldsymbol{f}$. They are supplemented by the gravitational force

$$\boldsymbol{f} = \rho \cdot \frac{GM_S}{r^2} \cdot \boldsymbol{n}_r \quad (5)$$

(G, gravitational constant; M_S, mass of the Sun; $\boldsymbol{n}_r$, unit vector along the radial direction) and the isothermal equation of state

$$p = 1.92\, N k_B T \quad (6)$$

(N, electron number density; k_B, Boltzmann's constant, T, temperature). The mass density ρ and the electron number density N are related by $\rho = 1.92\, \tilde{\mu} m_p N$ (m_p, proton mass) with the mean molecular weight $\tilde{\mu}$ (cf. e. g. Priest (1982)). In the solar corona and the solar wind $\tilde{\mu}$ has a value of 0.6 (Priest 1982). Here, stationary, spherical symmetric solutions of (2) and (3) are required. Thus, all quantities should only depend on the radial distance r from the center of the Sun. The magnetic field and the flow velocity are assumed to be radially directed, i. e., $\boldsymbol{B} = B(r)\boldsymbol{n}_r$ and $\boldsymbol{v} = v(r)\boldsymbol{n}_r$. Then, (2) can immediately be integrated to

$$r^2 \cdot N(r) \cdot v(r) = C \quad (7)$$

with the constant C and, subsequently, (3) transfers into

$$v \cdot \frac{dv}{dr} = -\frac{k_B T}{\tilde{\mu} m_p N} \cdot \frac{dN}{dr} - \frac{GM_S}{r^2} \quad (8)$$

Eliminating $N(r)$ in (8) by using (7), (8) can be integrated to

$$\frac{v(r)^2}{v_c^2} - \ln\left(\frac{v(r)^2}{v_c^2}\right) = 4 \ln\left(\frac{r}{r_c}\right) + 4 \cdot \frac{r_c}{r} - 3 \quad (9)$$

with the critical velocity $v(r = r_c) = v_c = (k_B T/\tilde{\mu} m_p)^{1/2}$ and the critical radius $r_c = GM_S/2v_c^2$ (cf. Priest (1982)). (9) represents the well-known *Parker*'s wind equation (Parker 1958). The density model $N(r)$ is found by substituting the solution $v(r)$ of (9) into (7). (9) has different solutions. Such a solution is chosen, which is continuously connecting the region of the solar corona, i. e., $r \ll r_c$, with the interplanetary space, i. e., $r \gg r_c$. Since v_c is the sound velocity, r_c represents the distance from the Sun, at which the solar wind becomes supersonic.

In the limit $v \ll v_c$, (7) and (9) can be solved analytically in terms of a barometric height formula

$$N(r) = N_S \cdot \exp\left[\frac{A}{R_S}\left(\frac{R_S}{r} - 1\right)\right] \quad (10)$$

with $A = \tilde{\mu} GM_S/k_B T$ and $N(r = R_S) = N_S$. R_S denotes the radius of the Sun. Note, that the well-known Newkirk (1961) model given by $N(r) = N_0 \cdot 10^{4.32 R_S/r}$ with $N_0 = 4.2 \cdot 10^4\ cm^{-3}$ corresponds to a barometric height formula with the temperature of $1.4 \cdot 10^4\ K$.

Table 1. The particle number density N_S (fourth column) at the bottom of the corona, i. e., 2300 km above the photosphere, the solar wind speed v_{1AU} (third column) as deduced from the numerical solutions of Eqs. (7) and (9) for different values of the temperature T (first column). The correspondig values of the critical radius r_c are given in the second column.

$T\ (10^6\ K)$	$r_c\ (R_S)$	$v_{1AU}\ (km\,s^{-1})$	$N_S\ (cm^{-3})$
2.0	3.43	674	$1.40 \cdot 10^7$
1.4	4.90	528	$1.61 \cdot 10^8$
1.0	6.91	427	$5.14 \cdot 10^9$

The constant C appearing in (7) is fixed by plasma in-situ measurements at 1 AU. At 1 AU a long duration average of the particle number density and the particle flux was found to be $N = 6.59\, cm^{-3}$ and $Nv = 2.8 \cdot 10^8\, cm^{-2} s^{-1}$ (Schwenn 1990), respectively, by means of the plasma data of the HELIOS 1 and 2 and IMP satellites. This results in a mean solar wind speed of 425 km s^{-1} at 1 AU. Thus, the constant C is determined to be $C = 6.3 \cdot 10^{34}\ s^{-1}$. Now, the temperature T is the only parameter appearing in (9). (7) and (9) are numerically evaluated for three values of T, i. e., $T = 1.0 \cdot 10^6\ K$, $1.4 \cdot 10^6\ K$, $2.0 \cdot 10^6\ K$. The results are summarized in Table 1. The third and fourth column contain the calculated values of the solar wind speed at 1 AU and the particle number density in the low corona, respectively. In the low corona, i. e., slightly above the transition region or 2300 km above the photosphere, a typical electron particle number density of $5 \cdot 10^9\ cm^{-3}$ is given by Vernazza et al. (1981). Inspecting Table 1, the solution of (7) and (9) with a chosen temperature of $1.0 \cdot 10^6\ K$ is in good agreement with the observed solar wind velocity of 425 km s^{-1} at 1 AU and the particle number density in the low corona (cf. Vernazza et al. (1981)).

Thus, the solution of (7) and (9) with $T = 1.0 \cdot 10^6\ K$, i. e., a special solution of *Parker*'s (1958) wind equation, is very compatible with the observations in the corona and the interplanetary space and can consequently be regarded as a reasonable global heliospheric density model. Fig. 1 shows the radial dependence of the particle number density N and the solar wind speed v according to (7) and (9) by choosing $T = 1.0 \cdot 10^6\ K$. The corresponding radial dependence of the electron plasma frequency f_{pe} is depicted in Fig. 2.

3. Discussion

Now, the heliospheric density model derived in the previous section and presented in Fig. 1 is compared with observations in the solar corona and the interplanetary space.

In Fig. 3 the density model (full line) is represented in the corona, i. e., in the range $r/R_S = 1.04$–1.30 or 28000–210000 km above the photosphere, in comparison with the fourfold Newkirk (1961) model, i. e., $N(r) = 4 \times N_0 \cdot 10^{4.32 R_S/r}$ with $N_0 = 4.2 \cdot 10^4\ cm^{-3}$. The Newkirk (1961) model resulted from measurements of white light scattering in the corona during a solar minimum period. The inspection shows, that the model agrees well with the fourfold Newkirk

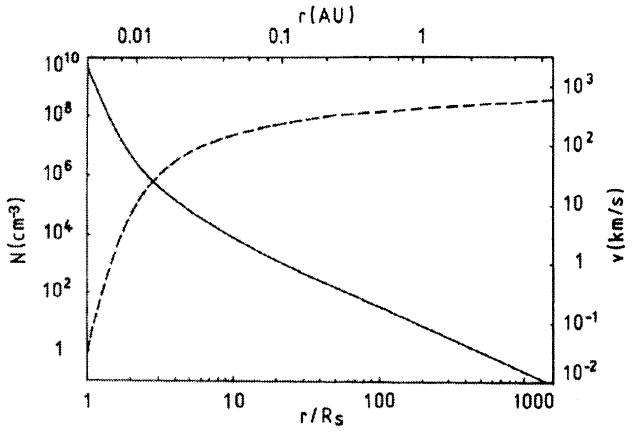

Fig. 1. Radial dependence of the particle number density $N(r)$ (full line) and the solar wind velocity $v(r)$ (dashed line) according to the numerical solution of Eqs. (7) and (9) with a temperature of $1.0 \cdot 10^6\ K$. The radial distance is given in terms of the solar radius $R_S = 6.958 \cdot 10^5\ km$ and astronomical units $1\ AU = 150 \cdot 10^6\ km$

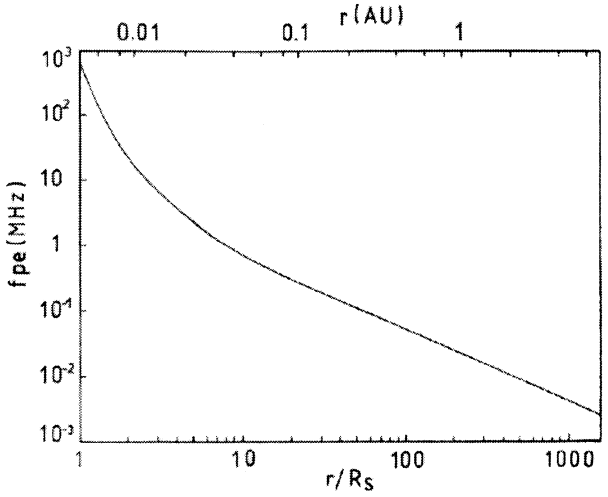

Fig. 2. Radial dependence of the local electron plasma frequency $f_{pe}(r)$

model within a mean error of 15%. The deviation between the Newkirk model and the model derived in this paper is growing beyond $1.3R_S$. Recently, Koutchmy (1994) reported on optical ground based measurements during the eclipse on July 11, 1991. The resulting radial behaviour of the electron density was presented in Fig. 4 of the paper by Koutchmy (1994) for coronal loops, streamers, quiet equatorial and polar regions. The density in these regions differ by three orders of magnitude. For example, a density of $2 \cdot 10^9\ cm^{-3}$, $8 \cdot 10^8\ cm^{-3}$, and $6 \cdot 10^6$ is found in coronal streamers, quiet equatorial and polar regions at a distance of $1.3R_S$ (cf. Fig. 4 in Koutchmy (1994)), respectively. At the same distance the model provides a density of $2.15 \cdot 10^8\ cm^{-3}$, which is the mean value of the density in the corona at this height.

The density behaviour in the outer corona and the interplanetary space was recently studied by the coronal radio sounding experiment at the ULYSSES spacecraft. Figs. 4 and 5 show the

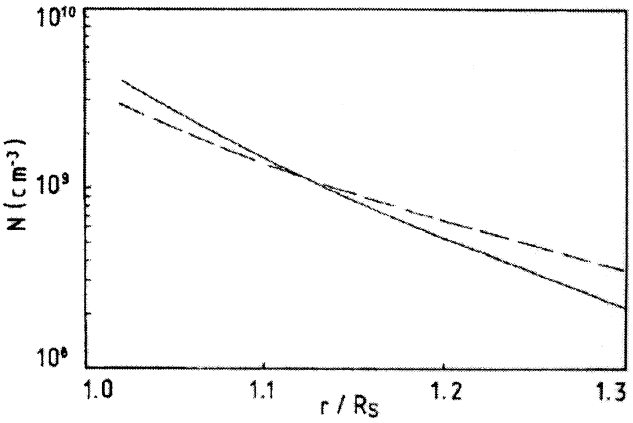

Fig. 3. Comparison of the particle number density $N(r)$ (full line) according to Fig. 1 and the fourfold Newkirk (1961) model (dashed line) in the range $1.02R_S - 1.30R_S$

radial behaviour of the particle number density in the range 5–$50R_S$ according to the model (full line) and the radio sounding measurements (dashed line) during the ingress phase (cf. Fig. 4) and egress phase (cf. Fig. 5) (Bird et al., 1994). The radio sounding measurements were perfomed by Bird et al. (1994) during the 1991 solar conjunction of the ULYSSES spacecraft. The ingress and egress phase cover a range 5–$35R_S$ and 5–$45R_S$, respectively. The inspection of the Figs. 4 and 5 reveals, that the model derived in Sect. 2 agrees well with the observations by ULYSSES in the range between $5R_S$ and $50R_S$. The deviation between the model and the measurements has a mean value of 18%.

Fig. 6 represents the radial density behaviour according to the model (full line) (cf. Sect. 2) in comparison with in-situ density measurements (dashed line) by the HELIOS 1 and 2 satellites (Bougeret et al., 1984) and the so-called RAE model (long dashed line) (Fainberg and Stone, 1971) in the range 0.1–$1.0\ AU$. Bougeret et al. (1984) derived a radial density model of the heliosphere by employing the in-situ density measurements during the period $1974 - 1980$. These observations are made in the range 0.3–$1.0\ AU$. The best fit of the data are obtained by $N(r) = 6.14 \cdot (r/R_{1AU})^{-2.10}$ in cm^{-3} for solar minimum conditions. The RAE model (Fainberg and Stone 1971) results from the investigation of type III bursts and type III radio storm bursts in the frequency range below 1 MHz by interplanetary radio measurements. Type III radio bursts appear as rapidly drifting emission stripes in dynamic radio spectra in the range $10\ \mathrm{kHz} - 300\ \mathrm{MHz}$. They are interpretated as the radio signature of sub-relativistic electron beams travelling from the solar corona along open magnetic field lines into the interplanetary space (cf. Suzuki and Dulk (1985) as a review). The model derived in Sect. 2 agrees well with the averaged data of the HELIOS in-situ measurements as demonstrated in Fig. 6. The deviation between the model by Bougeret et al. (1984) and our model has a mean value of 13%. On the other hand there is a great difference with the RAE model. This difference is not too surprising, since the RAE model (Fainberg and Stone 1971) is a indirectly derived model, i. e., it results from type III

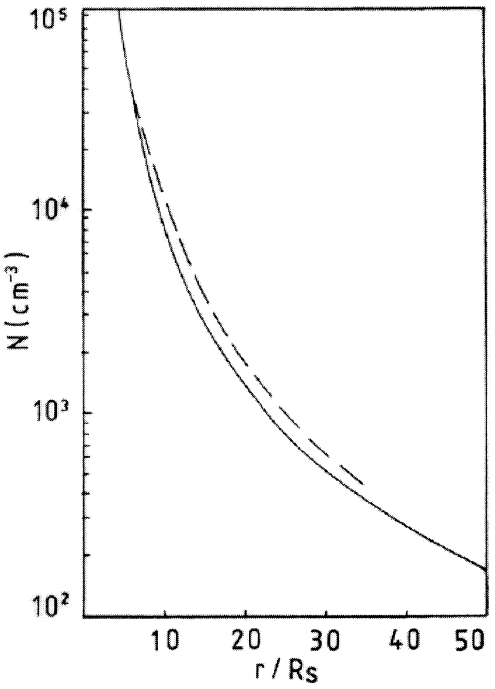

Fig. 4. Comparison of the density model (full line) (cf. Fig. 1) with the density measurements (dashed line) by the coronal radio soundig experiment (Bird et al. (1994)) of the ULYSSES mission during the ingress phase

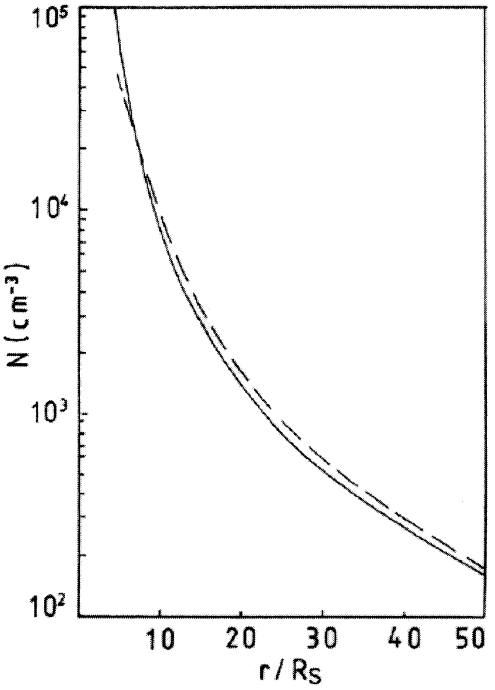

Fig. 5. The same format as displayed in Fig. 4 for the ULYSSES data during the egress phase (cf. Bird et al. (1994))

storm radio bursts measurements, while the model by Bougeret et al. (1984) uses the HELIOS in-situ measurements. Similar differences have been noted for other radio source locations (cf. e. g. Steinberg et al. (1984, 1985)). Robinson (1992) deduced a radial density behaviour of $N(r) \approx 7 \cdot (r/R_{1AU})^{-2.29}\ cm^{-3}$ from studying the radial variation of interplanetary type III burst source parameters. His result agrees with our model.

The radio instrument aboard the HELIOS satellite was able to localize the radio source in the interplanetary space. Kayser and Stone (1984) studied type III radio bursts and determined the source location of the different frequencies emitted during the movement of the electron beam in the interplanetary space. The result is presented in Table 2. Here, the radio waves are assumed to be predominantly emitted at the harmonic of the plasma frequency Thus, the particle number densities in the second column of Table 2 are calculated from the frequencies (left column of Table 2) by the assumption of harmonic emission. The corresponding radial source location obtained from the radio instrument aboard HELIOS is given in the third column. Thus, the frequency range $3\ \mathrm{MHz} - 26.5\ \mathrm{kHz}$ covers a range between $6R_S$ up to $374R_S = 1.73\ \mathrm{AU}$ ($1\ \mathrm{AU} = 214R_S$) in the heliosphere. The source location according to our model (cf. Sect. 2) is presented in the fourth column. The inspection of third and fourth column in Table 2 shows, that the model derived in Sect. 2 agrees very well with these observations over a great range in the heliosphere. The deviations between the observations and the model have a maximum and mean value of 15.2% and 11% (cf. right column in Table 2), respectively.

Table 2. Comparison of the radial source location of different plasma frequency levels (first column) as deduced by the radio measurements aboard HELIOS (third column) (cf. Kayser and Stone (1984)) and the model (fourth column) (cf. Sect. 2). The errors between the measurements and the model are given in the fifth column. The particle number densities (second column) are calculated by the assumption of harmonic emission.

$f(kHz)$	$N(cm^{-3})$	R/R_S HELIOS	R/R_S model	error %
3000	$2.79 \cdot 10^4$	6.0	6.51	7.8
2280	$1.61 \cdot 10^4$	7.7	7.75	6.5
1320	$5.40 \cdot 10^3$	12.5	11.58	7.9
1010	$3.16 \cdot 10^3$	15.7	14.31	9.7
765	$1.81 \cdot 10^3$	20.0	17.88	11.9
585	$1.06 \cdot 10^3$	25.4	22.30	13.9
445	$6.14 \cdot 10^2$	32.0	22.77	15.2
340	$3.59 \cdot 10^2$	40.6	35.53	14.9
255	$2.02 \cdot 10^2$	52.2	45.40	15.0
195	$1.18 \cdot 10^2$	65.8	57.33	14.4
150	$6.98 \cdot 10^1$	82.8	72.79	13.8
115	$4.01 \cdot 10^1$	104.3	92.49	12.8
85	$2.24 \cdot 10^1$	135.5	121.83	11.2
65	$1.31 \cdot 10^1$	171.1	155.91	9.7
50	7.75	215.0	198.70	8.2
26.5	2.18	373.5	358.88	4.1

At 5 AU our model provides a particle number density of $0.21\ cm^{-3}$, an electron plasma frequency of 4.15 kHz and a solar wind speed of 533 km s^{-1}. These values were also approximately found at 5 AU in the ecliptic plane by the ULYSSES satellite (Bame et al., 1992; MacDowall et al., 1996).

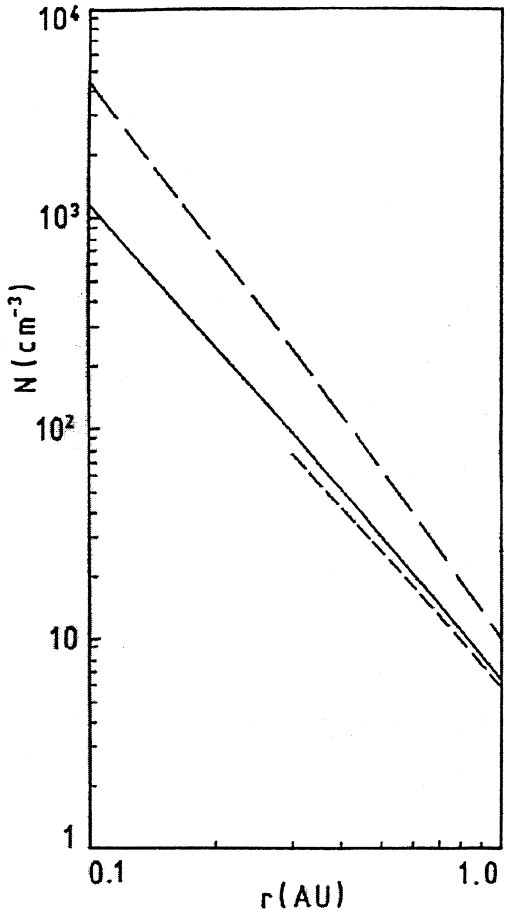

Fig. 6. Comparison of the density model (full line) (cf. Fig. 1) with the model by Bougeret et al. (1984) (dashed line) and Fainberg and Stone (1971) (long dashed line)

As already mentioned the radial density behaviour can be approximated by a barometric height formula (cf. (10)) in the corona. The analytical expression (10) is valid with $N_S = 5.14 \cdot 10^9\ cm^{-3}$ and $A/R_S = 13.83$ and represents an appropriate approximation of the solutions of (7) and (9) with a temperature of $1 \cdot 10^6\ K$ in the range 1.02–3.0R_S within an error of 2%. Thus, the electron plasma frequency f_{pe} behaves according to

$$f_{pe}(r) = f_S \cdot \exp\left[\frac{A}{2R_S}\left(\frac{R_S}{r} - 1\right)\right] \tag{11}$$

with $f_S = 644$ MHz. A plasma frequency of 6.4 MHz is calculated at $r = 3R_S$. The radial distance r of a level with the plasma frequency f_{pe} is deduced to be

$$r = \frac{R_S}{\left[1 + \frac{2R_S}{A} \cdot \ln\left(\frac{f_{pe}}{f_S}\right)\right]} \tag{12}$$

from (11). Then, a relationship between the drift rate D_f in dynamic radio spectra and the radial velocity V_r of the associated radio source

$$V_r = \frac{(-D_f)}{f} \cdot v_0 \cdot \left[1 + 0.145 \ln\left(\frac{f}{nf_s}\right)\right]^{-2} \tag{13}$$

can be found with $v_0 = 100620\ km$ by means of (1), (10), (11), and (12). On the other hand, the radial behaviour of the density can be approximated by

$$N(r) = N_{1AU} \cdot \left(\frac{r}{R_{1AU}}\right)^{-\alpha} \tag{14}$$

with $N_{1AU} = 6.53\ cm^{-3}$, $R_{1AU} = 150 \cdot 10^6\ km$, and $\alpha = 2.16$ beyound 0.2 AU. In the range 0.2–5.0 AU (14) reflects the behaviour of the derived density model within an error of 8%. This result agrees roughly with the density model by Bougeret et al. (1984) (cf. also Fig. 6). Using (1) and (14) the relationship between the drift rate D_f and the radial source velocity V_r

$$V_r = \frac{2(-D_f)}{f} \cdot \frac{R_{1AU}}{\alpha} \cdot \left(\frac{f}{nf_{1AU}}\right)^{-2/\alpha} \tag{15}$$

is found with $f_{1AU} = 23$ kHz. In (13) and (15) $n = 1$ and $n = 2$ should be used for the fundamental and harmonic emission, respectively.

In order to demonstrate the use of the density model derived in Sect. 2, it is applied for estimating the source velocity of solar and interplanetary type III radio bursts. As already mentioned type III radio bursts represent the radio signature of electron beams produced by solar flares and, subsequently, propagating along open magnetic field lines through the corona into the interplanetary space (cf. Suzuki and Dulk (1985) and Gurnett (1995) as a review). On December 27, 1994 a group of solar type III radio bursts have been observed by the radiospectrometer (40–800 MHz) (cf. Fig. 7) (Mann et al. 1992) of the Astrophysikalisches Institut Potsdam. They started at 170 MHz on 10:42:15 UT (cf. Fig. 7). The associated interplanetary type III burst extended to lower frequencies, i.e. up to 20 kHz, as recorded by the WAVES instrument (cf. Fig. 8) (Bougeret et al. 1995) and the URAP instrument (cf. Fig. 9) (Stone et al. 1992) aboard the WIND and ULYSSES spacecraft, respectively. The comparison of the Figs. 7, 8 and 9 suggests that the group of solar type III radio bursts was merging to a single interplanetary type III burst, i. e., the single electron beams produced in the low corona were merging to a giant electron beam in the interplanetary space. The measurements of the drift rates of these type III bursts in the dynamic radio spectra (cf. Figs. 7, 8, 9) reveals a relationship

$$D_f = -0.007354 f^{1.76} \tag{16}$$

between the drift rate D_f (in MHz s^{-1}) and the frequency f (in MHz) (cf. Fig. 10). The drift rates have been determined at the leading edge of the individual type III bursts. Thus, a mean drift rate of -18.3 MHz s^{-1} and -0.0255 kHz s^{-1} has been observed at 85 MHz and 40 kHz, respectively. In the corona the radio emission of type III bursts can take place near the fundamental or harmonic of the electron plasma frequency (Melrose 1985). Then, a radial velocity of 43000 km s^{-1} or 59000 km s^{-1} is found for the type III related electrons in the corona by (13) in the case of fundamental or harmonic emission, respectively. Furthermore, the radio radiation of interplanetary type III bursts is generally assumed to be emitted at the harmonic of the electron plasma frequency (Reiner et al. 1992). Then, the radial

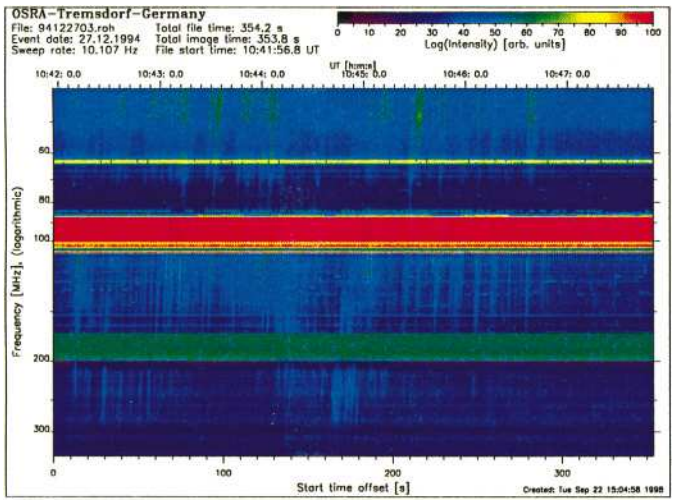

Fig. 7. Dynamic radio spectrum of the solar type III burst group on December 27, 1994 as recorded by the radiospectrometer (40−800 MHz) of the Astrophysikalisches Institut Potsdam

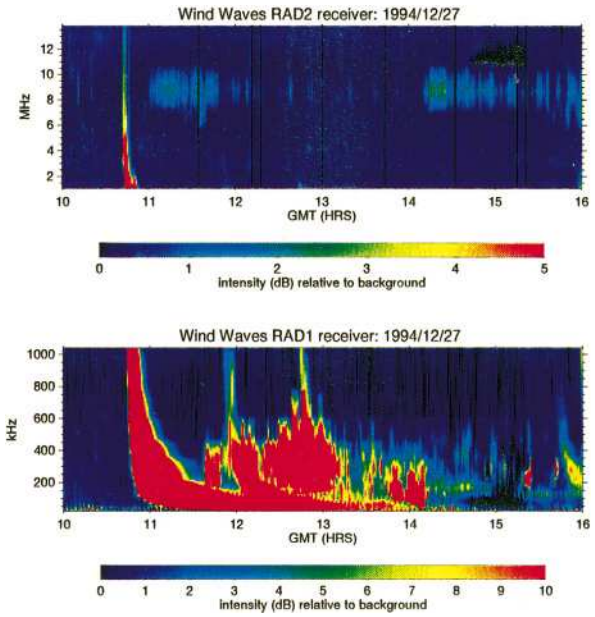

Fig. 8. Dynamic radio spectrum of the interplanetary type III burst on December 27, 1994 measured by the WAVES instrument aboard WIND. In the RAD2 plot, signals in the 8–10 MHz range are man-made terrestrial signals, broadened by the interpolation used to provide a continuous spectrum. In the RAD1 plot, the blotchy signals from 200–400 kHz are terrestrial kilometric radiation (TKR)

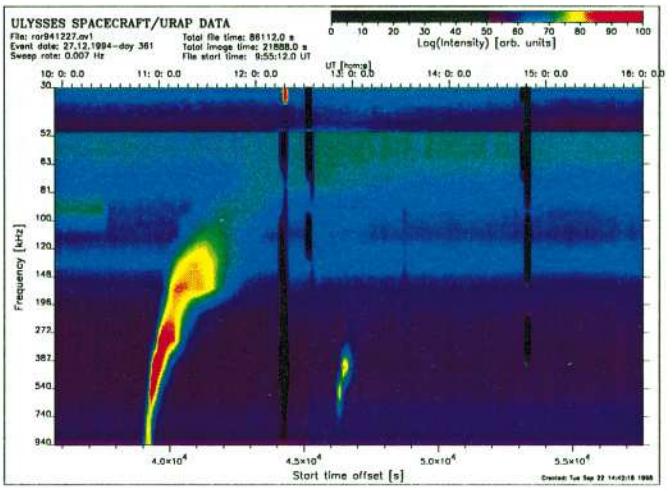

Fig. 9. Dynamic radio spectrum of the interplanetary type III burst on December 27, 1994 measured by the URAP instrument aboard ULYSSES

velocity of the type III burst related electrons is found to be about 100000 km s^{-1} (cf. (15)) at the 40 kHz level corresponding a radial distance of 1.14 AU from the Sun. On the other hand, Lin et al. (1996) measured the energy spectrum of these type III electrons by the 3D plasma instrument (Lin et al. 1995) aboard the WIND satellite on December 27, 1994. These electrons have energies in the range $1.323\,keV \leq E_{kin} \leq 109\,keV$ (cf. Lin et al. (1996)), which correspond to radial velocities V_r of 22000 $km\,s^{-1} \leq V_r \leq 170000\ km\,s^{-1}$. Thus, the beam, which is responsible for the type III burst on December 27, 1994 (cf. Figs. 7, 8, 9), has a broad energy spectrum. The radial velocities of the type III burst related electrons show that the slower electrons of the beam, i. e., $V_r \approx 50000\ km\,s^{-1}$, generated the type III burst in the MHz range, while the faster electrons with $V_r \approx 100000\ km\,s^{-1}$ are producing the interplanetary type III burst at 40 kHz. This can be explained in the following manner: As already mentioned the radio radiation is generated by Langmuir waves or upper hybrid waves (Melrose 1985). These high frequency electrostatic waves are produced by energetic electron beams "via a beam-plasma" instability. Such an instabiltity occur if the distribution function $f(V)$ of the electrons has a region with a positive slope, i. e., $\partial f/\partial V > 0$, (cf. Krall and Trivelpiece (1973)). (Here, V denotes the velocity of the electrons.) Initially, electrons with a broad energy spectrum are produced by a flare in the corona. The slower part of this electron ensemble is able to fulfill the above condition of instability. Consequently, these slow electrons are producing the solar type III burst. However these electrons are propagating along open magnetic field lines into the interplanetary space. Thus, the faster part of these electrons is running away, i. e., the fastest electrons are first to reach the interplanetary space (e. g. the 40 kHz level at 1.14 AU), where they produce the interplanetary type III burst. This scenario agrees well with the radio measurements presented in this paper and the measurements by Lin et al. (1996) (cf. Figs. 1 and 3 in Lin et al. (1996)).

The comparison between the density model (cf. Figs. 3–6) and different density measurements in the heliosphere, i. e., from the corona up to a distance of 5 AU in the interplanetary space, demonstrates that the model representing a special solution of *Parker*'s (1958) wind equation (9) reflects very well the radial density behaviour in the heliosphere, in particular, in the region near the ecliptic plane. The density model derived in Sect. 2 and illustrated in Figs. 1 and 2 should be regarded as a good approximation of the radial behaviour of the density in the heliosphere, although the heliosphere is spatially and tempo-

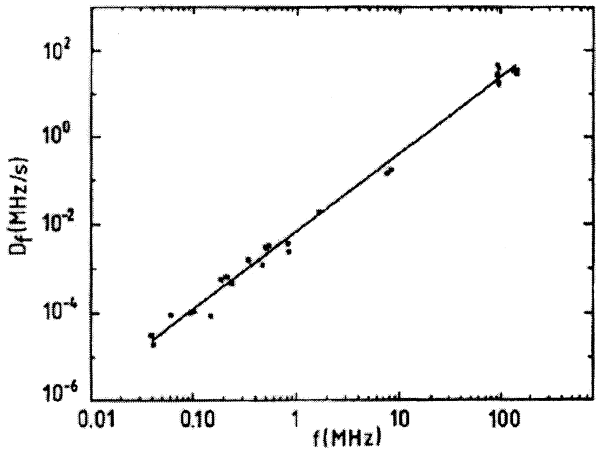

Fig. 10. The drift rate D_f versus the frequency F of the solar and associated interplanetary type III radio bursts on December 27, 1994 as derived from the dynamic radio spectra presented in Figs. 7, 8, and 9

rally varying with respect to the density (cf. Schwenn (1990)). Thus, this model is a useful tool for the interpretation of solar and interplanetary radio data, especially the determining of radial source velocities from drift rates (cf. (1) in dynamic radio spectra.

References

Bame S.J., Barraclough B.L., Feldman W.D., et al., 1992, Sci 257, 1539
Bird M.K., Volland H., Pätzold M., et al., 1994, ApJ 426, 373
Bougeret J.-L., Kaiser M.L., Kellog P.J., et al., 1995, In: Russell C.T (ed.) The Global Geospace Mission. Kluwer Acadameic Press, Dordrecht, p. 231
Bougeret J.-L., King J. H., Schwenn R., 1984, Solar Phys. 90, 401
Fainberg J., Stone R.G., 1971, Solar Phys. 17, 392
Gurnett D.A., 1995, Space Sci. Rev. 72, 243
Kayser S., Stone R.G., 1984, In: Porsche H. (ed.), 10 years HELIOS. Bonn, p. 111
Koutchmy S., 1994, Adv. Space Res. 14 (4), 29
Krall N.A., Trivelpiece A.W., 1973, Principles of Plasma Physics. McGraw-Hill, New York
Lin R.P., Anderson K.A., Ashford S., et al., 1995, Space Sci. Rev. 71, 125
Lin R.P., Larson D., Mc Fadden J., et al., 1996, Geophys. Res. Lett. 23, 1211
MacDowall R.J., Hess R.A., Lin N., et al., 1996, A&A 316, 396
Mann G., Aurass H., Voigt W., Paschke J., 1992, ESA-Journal SP-348, 129
Melrose D., 1985, In: McLean J.M., Labrum N.R. (eds.) Solar Radiophysics. Cambridge University press, Cambridge, p. 135
Newkirk G.A., 1961, ApJ 133, 983
Parker E.N., 1958, ApJ 128, 664
Priest E.R., 1982, Solar Magnetohydrodynamics. Reidel, Dordrecht
Reiner M.J., Stone R.G., Fainberg J., 1992, ApJ 394, 340
Robinson P.A., 1992, Solar Phys. 137, 307
Schwenn R., 1990, In: Schwenn R., Marsch E. (eds.) Physics of the Inner Heliosphere. Springer-Verlag, Berlin, Heidelberg, p. 99
Steinberg J.L., Dulk G.A., Hoang S., Lecacheux A., Aubier M., 1984, A&A 140, 39
Steinberg J.L., Hoang S., Dulk G.A., 1985, A&A 150, 205
Stone R.G., Bourgeret J.L., Caldwell J., et al., 1992, A&AS 92, 291
Suzuki S., Dulk G.A., 1985, In: McLean J.M., Labrum N.R. (eds.) Solar Radiophysics. Cambridge University press, Cambridge, p. 289
Vernazza J.E., Avrett E.H., Loeser R., 1981, ApJS 45, 635